

A. Khodabandeh, R. D. Arrua, B. R. Coad, T. Rodemann, T. Ohigashi, N. Kosugi, S. C. Thickett and E. F. Hilder

**Morphology control in polymerized high internal phase emulsion templated via macro-RAFT agent composition: visualizing surface chemistry**

Polymer Chemistry, 2018; 9(2):213-220

This journal is © The Royal Society of Chemistry 2018

Published at: <http://dx.doi.org/10.1039/c7py01770g>

**PERMISSIONS**

<http://www.rsc.org/journals-books-databases/journal-authors-reviewers/licences-copyright-permissions/#deposition-sharing>

**Deposition and sharing rights**

When the author accepts the licence to publish for a journal article, he/she retains certain rights concerning the deposition of the whole article. This table summarises how you may distribute the accepted manuscript and version of record of your article.

Sharing rights	Accepted manuscript	Version of record
Share with individuals on request, for personal use	✓	✓
Use for teaching or training materials	✓	✓
Use in submissions of grant applications, or academic requirements such as theses or dissertations	✓	✓
Share with a closed group of research collaborators, for example via an intranet or privately via a <a href="#">scholarly communication network</a>	✓	✓
Share publicly via a scholarly communication network that has signed up to STM sharing principles	⌚	×
Share publicly via a personal website, institutional repository or other not-for-profit repository	⌚	×
Share publicly via a scholarly communication network that has not signed up to STM sharing principles	×	×

⌚ Accepted manuscripts may be distributed via repositories after an embargo period of 12 months

**15 October 2019**

<http://hdl.handle.net/2440/114139>



## Morphology control in polymerised high internal phase emulsion templated via macro-RAFT agent composition: Visualizing surface chemistry

Received 00th January 20xx,  
Accepted 00th January 20xx

DOI: 10.1039/x0xx00000x

[www.rsc.org/](http://www.rsc.org/)

A. Khodabandeh,<sup>a,b</sup> R. D. Arrua,<sup>b</sup> B. R. Coad,<sup>c</sup> T. Rodemann,<sup>d</sup> T. Ohigashi,<sup>e</sup> N. Kosugi,<sup>e</sup> S. C. Thickett,<sup>f</sup> and E. Hilder<sup>b\*</sup>

A series of polymerized high internal phase emulsion (polyHIPE) materials have been prepared by using a water in oil emulsion stabilized by a macro-RAFT agent acting as a polymeric surfactant, 2-(butylthiocarbonothioylthio)-2-poly(styrene)-b-poly(acrylic acid). The pore structure of formed polyHIPEs were closed. By removing the RAFT-end group of the amphiphilic macro-RAFT agent, the obtained polyHIPE possessed an open structure with voids. The effect of the RAFT end-group of the amphiphilic macro-RAFT agent on the surface chemistry of the polyHIPE is discussed. The obtained polyHIPEs via this surfactant-assisted functionalization strategies were characterized by FTIR spectroscopy, FTIR mapping, SEM, SEM-EDX, TEM, XPS as well as synchrotron-based scanning transmission X-ray microscopy (STXM). The latter technique revealed the surface chemistry of the obtained polyHIPEs and macro-RAFT agent multicomponent with a surface spatial resolution of the order of 30-100 nm.

### Introduction

Polymerized high internal phase emulsions (polyHIPEs) are a class of macroporous, monolithic polymer materials, often with interconnected structures.<sup>1-3</sup> As these materials feature a high porosity and consequently, a low resistance to the mass transfer, they have been widely studied for potential applications in separation science.<sup>4, 5</sup> Polymer porosity, homogeneity and functionality are key design factors for a porous monolith to be considered as an effective separations medium. However, the control over such factors, and analytical methods for measuring chemical properties within pores or voids remains challenging.

Recently a new strategy for preparation of such monoliths, called “polymeric surfactant-assisted functionalization” has been established to offer a greater degree of control over the porosity of the obtained monolith. The synthesis of polyHIPE materials involves the use of polymeric surfactants prepared by reversible addition–fragmentation chain transfer (RAFT) polymerization. These well-defined and tunable amphiphilic diblock copolymers generate well-defined, porous monolithic structures possessing chemical functionality generated on the surface interface between the polymer and the voids.<sup>6</sup>

The RAFT technology has proved to be particularly versatile among the various reversible deactivation radical polymerization (RDRP) techniques. A series of amphiphilic macro-RAFT agents can be prepared not only to incorporate different types of hydrophilic and hydrophobic monomers, but controlled polymerisation allows one to incorporate the desired number of repeat units. This provides a comprehensive strategy for generating new amphiphilic surfactants that offer many advantages over conventional surfactants. The use of macro-RAFT agents has been demonstrated for the synthesis of hydrophilic surface modified styrene-based polyHIPEs by Mathieu *et al.*<sup>6</sup> From the same group, a series of polymerized medium internal phase emulsion (polyMIPEs) materials was

<sup>a</sup> Australian Centre for Research on Separation Science (ACROSS), University of Tasmania, Tasmania, Australia

<sup>b</sup> Future Industries Institute, University of South Australia, Building X, Mawson Lakes Campus, GPO Box 2471, Adelaide SA 5001, Australia

<sup>c</sup> School of Agriculture, Food and Wine, University of Adelaide, Adelaide SA 5005, Australia

<sup>d</sup> Central Science Laboratory, University of Tasmania, Private Bag 74, Hobart 7001, Australia

<sup>e</sup> Institute for Molecular Science, Okazaki 444-8585, Japan

<sup>f</sup> School of Physical Sciences, University of Tasmania, Private Bag 75, Hobart 7001, Australia

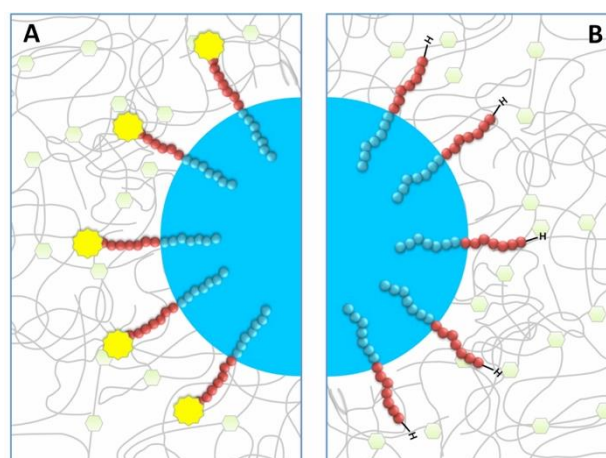
Electronic Supplementary Information (ESI) available: [details of any supplementary information available should be included here]. See DOI: 10.1039/x0xx00000x

stabilized by using the same macro-RAFT agent. The polyHIPE structure was studied in order to find the main parameters that influence the size of the voids and the windows of the porous monolith.<sup>7</sup> To understand the surface chemistry they used an indirect method, (static water contact angle measurements) which is related to the interfacial energies between the water droplet and surface of the material. Another example of using macro-RAFT agents in polyHIPE synthesis was demonstrated by Luo *et al.*, where the hydrophilic block of the macro-RAFT agent on the surface of polyHIPE was characterized by X-ray photoelectron spectroscopy (XPS) method.<sup>8</sup> In general, XPS analysis has been widely used for surface characterization of polyHIPEs.<sup>9-15</sup> While this technique provides details of surface chemistry, the spatial resolution of the technique is only slightly better than fluorescence microscopy,<sup>16</sup> meaning that that precise chemical information within micrometre-sized pores is beyond the spatial resolution of XPS.

In our previous study, a macro-RAFT agent was used as an anionic emulsifier in an inverse (oil in water) HIPE approach.<sup>17</sup> The surface chemistry of the obtained polyHIPE was mapped using RAMAN spectroscopy. Further, we explored the PEO-based brush-type amphiphilic macro-RAFT agents as sole emulsifiers in stabilizing inverse HIPE templates, which upon polymerization resulted in a PolyHIPE which was subsequently investigated as stationary phase for liquid chromatography [Reference].

Our group seeks to develop straightforward, one-pot functionalization methods to create porous monolith materials with multiple components relevant to separation science applications. We specifically target the ability to control the morphology and functionality of porous monolithic materials possessing a homogeneous structure.<sup>18-20</sup> In this study, generated polyHIPEs template from water-in-oil emulsion polymerisations using anionic RAFT-derived diblock copolymers as emulsifiers. For the characterization of such porous monoliths, visualizing surface chemistry at the nanoscale is imperative. During polyHIPE formation, we hypothesise that our polymeric surfactant copolymers remain on the surface of polyHIPE structure either through physi- or chemisorption (Scheme 1). Herein we test and evaluate this hypothesis using synchrotron-based scanning transmission X-ray microscopy

(STXM), a new technique for the characterization of polyHIPE monoliths, providing surface spatial resolution on the order of 30-100 nm.



**Scheme 1** Schematic representation of the PolyHIPE polymerization approach towards straightforward surface functionalization by acrylic acid (AA). A) Using a macro-RAFT agent and B) using an end-group removed macro-RAFT agent as sole emulsifier. The large blue circle represents the aqueous phase, small blue circles are AA units, red circles are styrene units and the yellow star represents the RAFT moiety of the macro-RAFT agent.

## Experimental Section

### Materials

Styrene (Sty, Aldrich, 99%) was passed through a column of Al<sub>2</sub>O<sub>3</sub> to remove the inhibitor. Acrylic acid (AA, Merck, ≥99%) was purified by distillation under reduced pressure. The RAFT agent, 2-[[[(butylsulfanyl)-carbonothioyl]sulfanyl] propanoic acid (PABTC), was synthesized as described in Ref.<sup>21</sup> Methanol (Fluka), basic alumina (Al<sub>2</sub>O<sub>3</sub>, Brockman activity I, 60-325 mesh), calcium chloride dihydrate (CaCl<sub>2</sub>, APS Ajax Finechem, 98%), 4,4'-azobis(4-cyanovaleric acid) (V501, >98%, Aldrich) were all used as received. 2, 2'-azobis(isobutyronitrile) (AIBN, MP Biomedicals, Eschwege, Germany) was recrystallized from methanol.

### Synthesis of amphiphilic surfactant by RAFT polymerization

A series of amphiphilic quasi-block macro-RAFT agents (Qb) consisting of AA and Sty were synthesised by some modification as reported in the literature.<sup>8</sup> A typical polymerization protocol

that was adopted is summarized: 1 g ( $4.20 \times 10^{-3}$  mol) of PABTC and 0.12 g ( $4.20 \times 10^{-4}$  mol) of V501 were introduced to a round-bottom flask which was then sealed with a rubber septum, and solids were purged with argon for 10 min. Then 1.82 g ( $2.52 \times 10^{-2}$  mol) of acrylic acid (AA) was then dissolved in 50 mL of dioxane before addition to a flask to obtain a solution. This was purged with argon for 10 min. The reaction was allowed to proceed at 80°C for 3 h under constant stirring. After quenching the reaction in an ice bath, a small aliquot of the solution was removed for  $^1\text{H}$  NMR analysis. Styrene (Sty) and V501 were then added to the round bottom flask at a molar ratio (relative to the initial chain transfer agent concentration) equal to the desired number of monomer repeat units per macro-RAFT agent. The mixture was further purged with argon for 10 min and further polymerization for 12 h at 80°C was performed. After which a small aliquot of the solution was removed for SEC and  $^1\text{H}$  NMR analysis.

The product (Macro-RAFT agent) was collected by precipitation of the above mixture in water and then water was removed via freeze-drying at  $-30$  °C under reduced pressure for at least 100 hours (see ESI Fig. S1†). To investigate the effect of the RAFT moiety, the RAFT part of the macro-RAFT agents were cleaved using a typical protocol with minor modifications (see Table 1 and ESI). The polymer was then stored at 4 °C until used. Fig. 1 shows the general synthesis of  $\text{AA}_m\text{-b-Sty}_n$  quasi-block copolymers. Table 1 shows the characteristic data for the  $\text{P}(\text{AA})\text{-qb-P}(\text{Sty})$  diblock copolymers synthesized in this study.

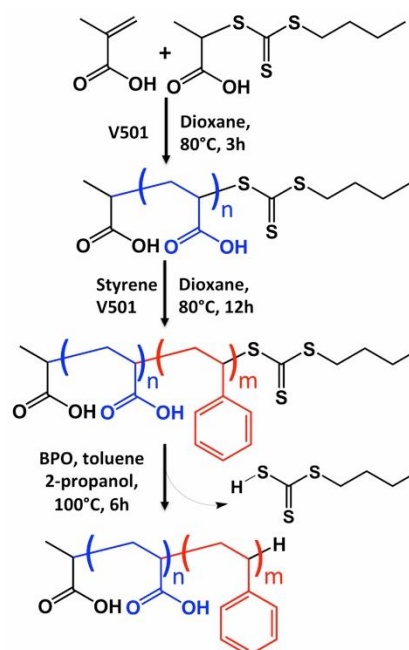


**Fig. 1** General synthesis of the  $\text{P}(\text{AA})\text{-qb-P}(\text{Sty})$  amphiphilic quasi-block copolymers

**Table 1.** Amphiphilic surfactant synthesized in this study

$(\text{AA})_x\text{-qb-(Sty)}_y$	X (feed) (AA) <sup>a</sup>	Y (feed) (Sty) <sup>a</sup>	$M_{n, \text{SEC}}$ (g mol <sup>-1</sup> )	$\bar{D}$
<b>Qb-1</b>	6	12	1291	1.19
<b>Qb-2</b>	3	6	1015	1.12
<b>End group removed-Qb-1</b>	6	12	1245	1.19
<b>End group removed-Qb-2</b>	3	6	902	1.12

<sup>a</sup>Determined by SEC in THF (Calibration Sty). Detailed polymerization conditions are provided in Table S1.

#### Polymerization of styrene-based polyHIPEs

A desired concentration of the quasi-block copolymer (surfactant) and AIBN (initiator) were dissolved in styrene and divinylbenzene (oil phase monomers). The aqueous phase containing calcium chloride (to suppress the Ostwald ripening) was added drop-wise to the oil phase at a rate of 0.8 mL min<sup>-1</sup> with constant stirring at 1000 rpm. Then, the emulsion was stirred at 14000 rpm using homogenizer for 2 minutes (Ultra Turrax T 25 IKA, 7.5 mm rotor, Germany). The emulsion was transferred to a mold (a glass container) and cured in a water bath at 65 °C for 24 h. The resulting polyHIPE was purified via Soxhlet extraction with methanol for 48 h as well as 48 hours with water. The purified monolith was dried in a vacuum oven

at 30 °C for at least 72 h to constant weight. Four different types of polyHIPEs were prepared by varying the type of quasi-block copolymers used in the polymerization process. The experimental conditions used for the preparation of the different polyHIPEs can be found in Table 2.

**Table 2.** Morphological features of polyHIPE samples.

Sample code	macro-RAFT agent	%wt	(SEM) ( $\mu\text{m}$ )	
			<D> <sup>(1)</sup>	<d> <sup>(1)</sup>
A1	Qb-1	10	5.35	-
A2	Qb-2	10	4.39	-
A3	End group removed Qb-1	10	-	-
A4	End group removed Qb-2	10	4.65	0.81

<sup>(1)</sup>A void describes the pores of the PolyHIPE and <D> is average size of voids. Window refers to the interconnecting pores between two adjacent droplets and <d> is average size of windows.

#### Characterization techniques

NMR analyses was performed using a Bruker Ultra Shield Avance Spectrometer (600 MHz). For all NMR analyses deuterated solvents were used as stated. Size exclusion chromatography (SEC) was performed using a Viscotek instrument using a refractive index detector (RID) and two chromatography columns (two PSS S linear 3  $\mu\text{m}$ , Polymer Standard Services GmbH, PSS) and THF (HPLC grade) as eluent (flow rate 0.5 mL min<sup>-1</sup>). The column oven was kept at 40 °C. All polymer samples were dissolved overnight in the eluent at a concentration  $\sim$  2 mg mL<sup>-1</sup>, then filtered through a 450 nm Nylon filter. The calculated molecular weights were based on calibration with respect to polystyrene (PSt) standards spanning a mass range of 160 to 154000 g mol<sup>-1</sup> (PSS-Polymer Laboratories). The standards were prepared (2 mg mL<sup>-1</sup>) and injected.

PolyHIPEs were characterized by field emission gun scanning electron microscopy (FE-SEM) studies using a Hitachi SU-70 FESEM in the Central Science Laboratory, University of Tasmania. All samples were platinum coated for 15 s in an argon atmosphere (Emitech 550, Emitech Ltd., UK). The calculation of the average pore and windows diameter (in the case of any) was performed on sets of at least 100 pores and 100 windows, respectively, using the image analysis software ImageJ (NIH

image).<sup>22</sup> A statistical correction was employed to obtain more accurate value by using a correction factor of  $2/(3^{1/2})$ , as described by Carnachan *et al.*<sup>23</sup>

The composition of the material was examined by EDX experiments where the materials were sputter-coated with carbon (Ladd 40000 carbon evaporator) before analysis. Sulfur content was analyzed using CHNS elemental analysis using a Thermo Finnigan EA 1112 Series Flash Elemental Analyser. The sample mass was about 15 mg. FTIR spectra were recorded using a Bruker Vertex 70 infrared spectrometer equipped with an ATR probe coupled with a Hyperion 3000 (FPA - microscope). X-ray photoelectron spectroscopy (XPS) was performed on a Kratos Axis Ultra DLD equipped with a monochromatic Al K $\alpha$  source (1486.6 eV). Each sample was analysed at an emission angle normal to the sample surface. Wide-scan spectra (1100 – 0 eV) were acquired at a pass energy of 160 eV and high resolution C 1s spectra were acquired at 20 eV. Data were processed with CasaXPS (ver.2.3.16 Pre rel. 1.6, Casa Software Ltd). Bright field TEM images were obtained at the McMaster Faculty of Health Sciences electron microscopy facility using a JEOL 1200EX operating at 80 kV.

STXM measurements were performed using the STXM at the BL4U beamline at the UVSOR Synchrotron (Okazaki, Japan). This instrument has been described previously in Ref.<sup>24</sup> After introducing the sample into the main STXM chamber, the chamber was evacuated and was filled with helium gas to 60 mbar. The STXM measurements in this case required  $\sim$  2 h of beamtime and a further 2 h of data analysis. The transmitted intensity (I) of the particles or reference materials was normalized by the transmitted intensity (I<sub>0</sub>) through Si<sub>3</sub>N<sub>4</sub> windows without the sample to yield the optical density OD = -ln(I/I<sub>0</sub>). All STXM data analysis was performed using the aXis2000 software provided by Adam Hitchcock.<sup>25</sup>

Techniques for preparing the thin section samples are similar to those used for transmission electron microscopy. Briefly, the polyHIPE was embedded with an aliphatic epoxy resin consisting of a 1:1 mixture of trimethylolpropane triglycidyl ether (TTE) and an alicyclic amine, 4,4'-methylene bis (2-methylcyclohexylamine) (MMCA), and was cured overnight at 60 °C. The embedded sample was then ultramicrotomed at

room temperature into  $\sim 100$  nm thin sections which were floated on distilled water and picked up onto Formvar-coated 100 mesh Cu TEM grids.

## Results and discussion

### Morphology control in polyHIPEs via macro-RAFT agent composition

In order to determine the influence of the RAFT moiety of the macro-RAFT agents on the morphology and the surface chemistry, control polyHIPEs A1 and A2 were synthesized using the macro-RAFT agent Qb-1 and Qb-2 (10% w.r.t. the continuous phase), respectively. Both polyHIPEs A1 and A2 possessed a closed morphology with average void diameters of  $5.35 \mu\text{m}$  and  $4.39 \mu\text{m}$ , respectively (Fig. 2 and Table 2). While the hydrophilic-hydrophobic balance (HLB number) of both macro-RAFT agents is the same, the lower molecular weight macro-RAFT agent was able to stabilize HIPEs with a smaller droplet size and as result of that a smaller voids in the obtained polyHIPE A2.

Further, by using the end group removed-Qb-1 (10 wt%) as a sole stabilizer, the successful stabilization of HIPE (A3) was obtained. Both the water droplet size and the morphology of the obtained polyHIPE differed relative to A1. A SEM image of the obtained polyHIPE is shown in Fig. 2. In comparison to polyHIPE A1, polyHIPE A3 possess an interconnected polyHIPE structure with an increased number of windows. The end group removed-Qb-2 (10 wt%) was also used as sole stabilizer but there was rapid phase separation, indicating an important role for the RAFT end group in stabilizing the system (See Fig. S2 †). It has been shown previously that reducing the interfacial initiation of the emulsion templated polymerization by removing the RAFT moiety has a significant effect on porosity of the resultant polyHIPE.<sup>6</sup> They observed that removing the RAFT moiety of a nonionic polymeric surfactant resulted in materials with an open structure; here we demonstrate the same trend with an anionic polymeric surfactant.

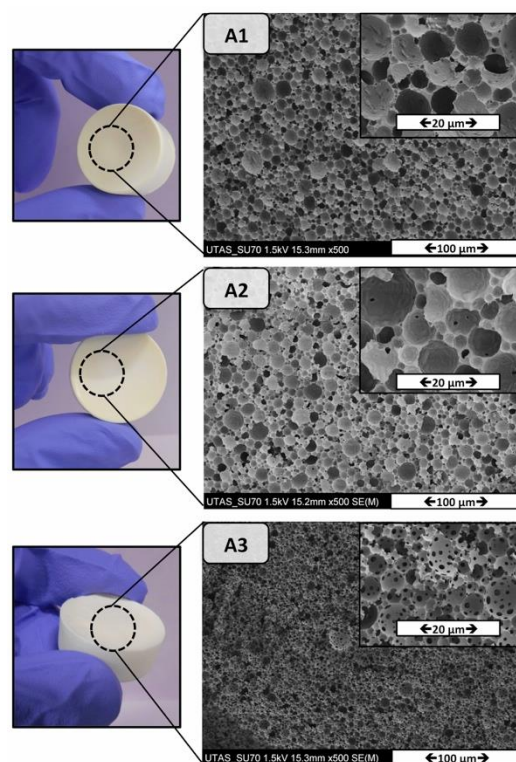


**Fig. 2** Scanning electron micrographs of emulsion template macroporous polymer made by polymerization of HIPEs stabilized solely by A1) macro-RAFT agent-Qb1, A2) macro-RAFT agent-Qb1, and A3) end group removed-Qb-1 at  $65 \text{ }^\circ\text{C}$  in presence of AIBN as initiator.

### Composition of polyHIPE containing quasi-block copolymers

It has been reported that the presence of the RAFT-end group in amphiphilic copolymers increases the hydrophobicity of the copolymer.<sup>26</sup> To further investigate the inclusion of the quasi-block copolymer within the polyHIPE structure, FTIR analyses were performed on the resultant materials, in comparison to a sample of Styrene-DVB polymerized in bulk (AIBN as initiators) subjected to the same washing protocol. A difference between the bulk polymer and polyHIPE A1 and A3 was found (Fig. S3 †). FTIR mapping confirmed the presence of the C=O groups in the same physical location as the walls of the polyHIPE voids, which are solely due to the carboxylic group of the acrylic acid segment (Fig. 3).

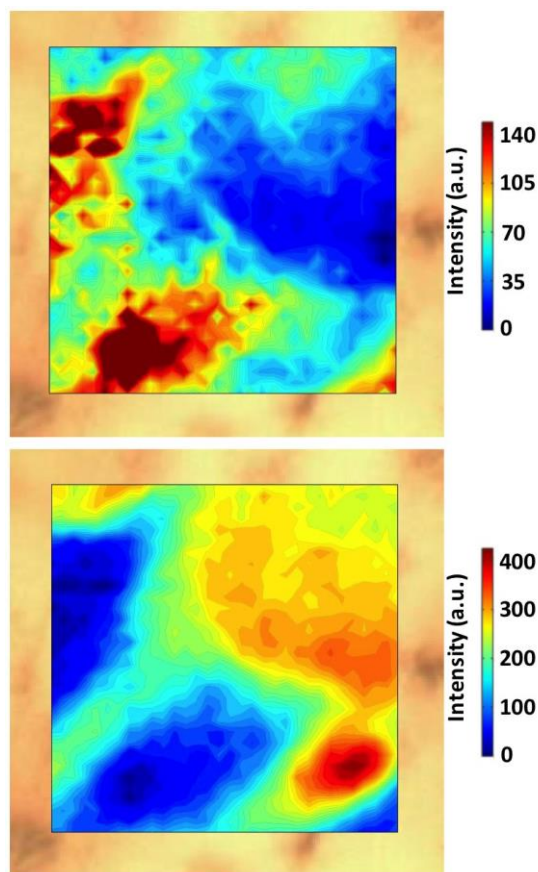


**Fig. 3** FTIR mapping (upper) based on the normalized carboxylic peak: (C=O/C=C) ( $1725 - 1770 \text{ cm}^{-1}$ ) peak area divided on aromatic carbon-carbon double bond peak area ( $2800 - 3000 \text{ cm}^{-1}$ ). FTIR mapping (bottom) based on signal to baseline from  $2800$  to  $3000 \text{ cm}^{-1}$  at the same area (dark blue regions in the lower image are void locations within the polyHIPE). The size of the image of the FTIR maps is  $30 \times 30 \mu\text{m}$ .

Further evidence for the presence of the macro-RAFT agent on the surface of the polyHIPE was obtained from Energy Dispersive X-ray analysis (EDX), clearly indicating that oxygen was present at the surface of the polyHIPE A3 (Fig. 4). The most likely explanation for this observation is that the quasi-block copolymer (or end-group removed Qb-1) was adsorbed to the surface of the polyHIPE A3. For polyHIPE A1, sulfur and oxygen were present originating from macro-RAFT agent Qb-1. Calcium and chloride (from  $\text{CaCl}_2$ ) were also present on the surface. This shows that the washing protocol for the closed-structure polyHIPE A1 was not able to wash out the co-stabilizer (see ESI Fig. S4 †). Elemental analysis also confirmed the presence of sulfur within the polyHIPE A1 (see Table S2 †).

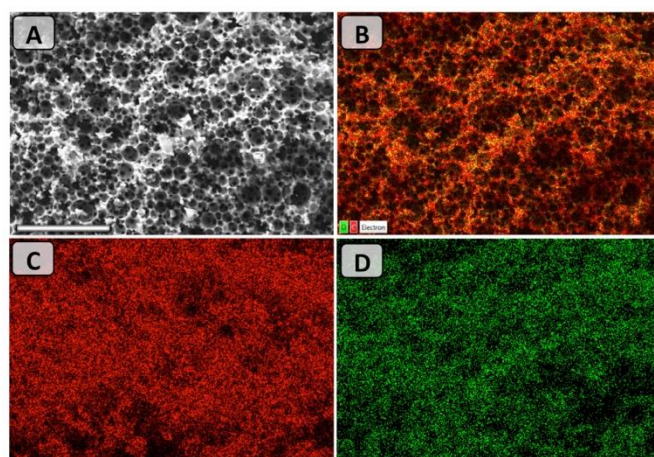


**Fig. 4** EDX mapping analysis on polyHIPE A3; (A) SEM image and (B) Overall mapping elements on the same spot: corresponding to carbon (C), and oxygen (D) mapping. Scale bar is  $50 \mu\text{m}$ .

In addition to the EDX-SEM and elemental analysis results, which show evidence for attachment of the quasi-block copolymer on the surface of polyHIPEs, polyHIPEs A1 and A3, and poly(styrene-co-DVB) were further evaluated by X-ray Photoelectron Spectroscopy (XPS). For A1, a large abundance of C (82%) and O (15%) was detected in the wide-scan elemental survey spectrum, as well as a small amount of S (0.6%) as expected. Additionally, there was evidence for trace amounts of Ca and Cl from the synthesis and adventitious Si from contamination. The high-resolution C 1s spectrum for PolyHIPE A1 was obtained and peak fitting was performed as shown in Fig. 5.

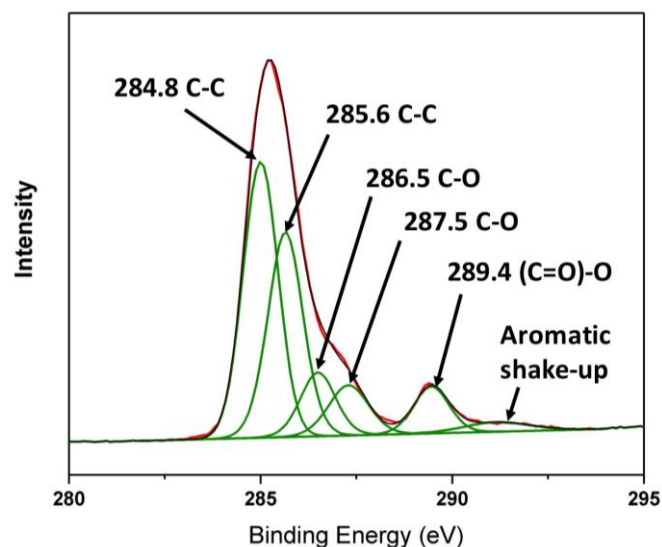


**Fig. 5** High-resolution C 1s spectrum for polyHIPE A1. Carbon binding environments (individually in green peaks with summed trace in red) were fit to the spectrum envelope (black).

Components could be fit to carboxylic acid and aromatic functionalities, as is consistent with the polymer structure. In contrast, the PolyHIPE A3 spectrum had a higher abundance of carbon, and lower abundance of oxygen (C = 95.4 %, O = 3.9 %) which was quantitatively and qualitatively similar to the spectrum for bulk styrene-DVB. As ejected photoelectrons originate from the outermost 10 nm of the sample, XPS analysis indicates a higher surface presentation of aromatic groups in the A3 sample compared to the A1 sample.

#### PolyHIPE Characterization by Scanning Transmission X-ray Microscopy (STXM)

A drawback in all characterization methods in the previous section is the limited spatial resolution making it difficult to probe the surface chemistry with the porous polyHIPE structure. In our group, scanning transmission X-ray microscopy (STXM) has been shown to be a powerful imaging technique that provides chemical selectivity and high spatial resolution of the order of  $\sim 35$  nm for the characterization of monoliths as support phases for liquid chromatography.<sup>19</sup> STXM is a synchrotron-based technique which combines near edge X-ray absorption fine structure (NEXAFS) spectroscopy and soft X-ray scanning microscopy. Chemical contrast is obtained from differences in NEXAFS carbon K-edge spectra, which arise due to differences in the  $\pi^*$  anti-bonding orbitals of the blend materials.<sup>27</sup> This powerful technique provides a relatively rapid chemical imaging of polymers using a sequence of highly resolved X-ray photon, enabling excellent spatial resolution and providing the possibility for quantitative analysis.<sup>28-30</sup>

STXM imaging was conducted by focusing on the C 1s core-line signal in NEXAFS. This region was selected because the aromatic chemical environment of carbon atoms is of particular interest for the present system. Fig. 6 shows the C 1s NEXAFS spectra obtained for both polyHIPEs (A1 and A3) and polystyrene cross-linked polyHIPEs. For these polyHIPEs TEM images are also shown in Fig. S5<sup>†</sup>.

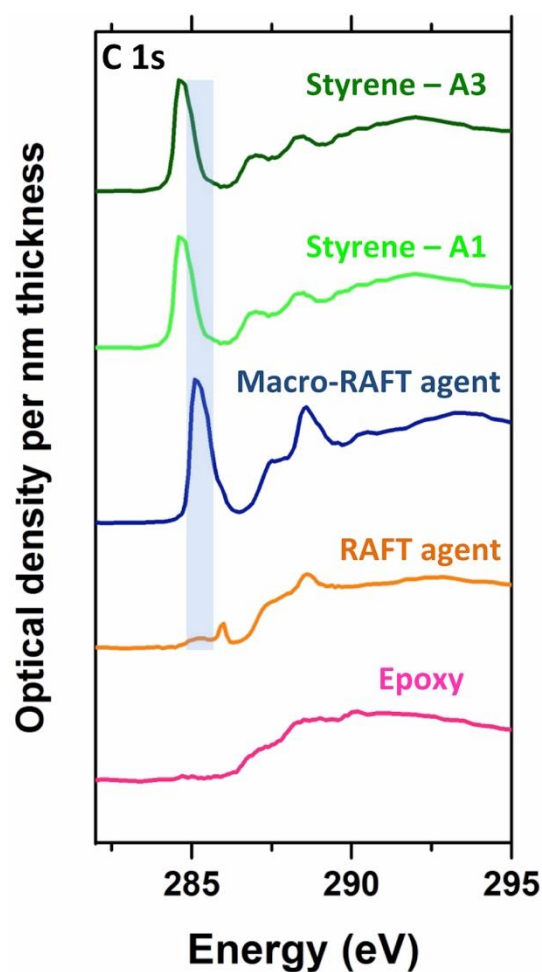


**Fig. 6** NEXAFS reference spectra of the epoxy (embedding matrix), RAFT agent, macro-RAFT agent, and polystyrene cross-linked polyHIPEs that correspond to 1 nm thickness of each component.

Reference spectra of the pure polymeric components were recorded with the same instrument: macro-RAFT agent Qb-1, RAFT agent (PABTC) and the epoxy resin which was used to embed the polyHIPEs. The components found by STXM were the poly(Sty-co-DVB) polyHIPE, the macro-RAFT agent, and the embedding resin. The spectrum for the crosslinked styrene-based scaffold has a strong peak at 284.6 eV, which is characteristic of C 1s  $\rightarrow \pi^*C=C$  transition in a phenyl ring. The macro-RAFT agent spectrum shows two peaks: a strong peak at 284.9 eV, which corresponds to the C 1s  $\rightarrow \pi^*C=C$  transition of the phenyl ring (styrene of macro-RAFT agent) and a peak at 288.9 eV, which is characteristic of C 1s  $\rightarrow \pi^*C=O$  transition in esters. In comparison to the RAFT agent spectrum, the intensity of peak at 288.9 eV increased due to acrylic acid incorporation in the macro-RAFT agent. It is also important to mention that



epoxy resin has little or no absorption at these energies and therefore provided excellent contrast between the resin, the scaffold, and the macro-RAFT agent.

Using a sequence of highly resolved X-ray photon energies covering the C 1s spectral region (280 to 320eV), successive images were obtained for polyHIPEs A1 and A3. Spectra for reference materials (macro-RAFT agent Qb1, Styrene-DVB, and epoxy) were color-coded and allowed for mapping of indicative chemical groups onto the image. The micrograph for polyHIPE A3 is shown in Figure 7. It can be seen clearly that the macro-RAFT agent (blue) is present at the interface between the void and scaffold. Here, the void was filled by the embedding matrix (epoxy in red). For polyHIPE A1, the STXM composite component map is shown in Fig. S6†. This image shows the same features as polyHIPE A3 indicating the chemical modification of the voids at the interface.

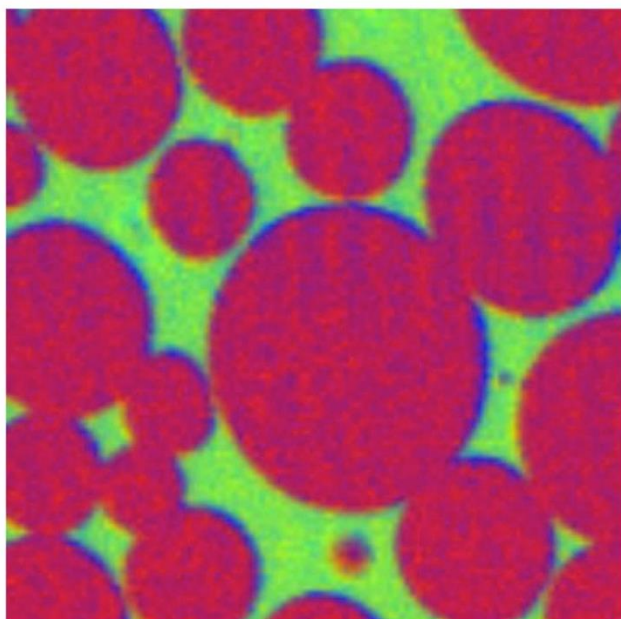


**Fig. 7** STXM color coded composite map (PolyHIPE A3, red=epoxy, green=PSty, blue=macro-RAFT agent).

## Conclusions

A hydrophilic coating was introduced to the poly(Styrene-DVB) polyHIPE materials by using a straight forward strategy which anchored poly(acrylate) to the surface. The pore size of the polyHIPEs was tunable by tailoring the macro-RAFT agent composition: These possessed closed structures when the HIPE

was stabilized by the macro-RAFT agent, and possessed open homogenous polyHIPE template materials when the RAFT agent of the amphiphilic macro-RAFT agent was cleaved prior stabilizing the HIPE. The surface chemistry of the polyHIPE materials was revealed by FTIR mapping as well as STXM.

Soft X-ray microscopy images recorded at multiple wavelengths were used to qualify the chemical composition in polyHIPE. This methodology was found to be effective for spectroscopically mapping the distribution of chemical functionalities of the macro-RAFT agent on the surface of macroporous polyHIPE monolith. The results shown in this work clearly demonstrate how STXM analysis can reveal chemical information for these materials.

## Acknowledgements

This work was supported by the Australian Research Council's Discovery funding scheme (DP130101471). E.F.H. is the recipient of an ARC Future Fellowship (FT0990521). The authors would like to acknowledge the Australian Commonwealth Government for an International Postgraduate Research Scholarship (IPRS) awarded to A.KH. We gratefully acknowledge Dr. James Horne for assistance with NMR, Dr. Karsten Gömann and Dr. Sandrin Feig for assistance with scanning electron microscopy (Central Science Laboratory, University of Tasmania). We are also thankful to Marcia Reid, Electron Microscopy Facility, McMaster University, Hamilton, ON, Canada, and Mr Yuichi Inagaki (Institute for Molecular Science, Japan) for assistance with preparation of the polyHIPE samples for STXM experiments.

## Notes and references

1. N. R. Cameron and D. C. Sherrington, *Adv. Polym. Sci.*, 1996, **126**, 163-214.
2. M. S. Silverstein, *Polymer*, 2014, **55**, 304-320.
3. M. S. Silverstein, *Prog. Polym. Sci.*, 2014, **39**, 199-234.
4. D. Wu, F. Xu, B. Sun, R. Fu, H. He and K. Matyjaszewski, *Chem. Rev.*, 2012, **112**, 3959-4015.
5. R. D. Arrua, T. J. Causon and E. F. Hilder, *The Analyst*, 2012, **137**, 5179-5189.
6. K. Mathieu, C. Jerome and A. Debuigne, *Macromolecules*, 2015, **48**, 6489-6498.
7. K. Mathieu, C. Jérôme and A. Debuigne, *Polymer*, 2016, **99**, 157-165.
8. Y. Luo, A.-N. Wang and X. Gao, *Colloid and Polymer Science*, 2015, **293**, 1767-1779.

9. Y. Zhang, J. Pan, Y. Chen, W. Shi, Y. Yan and L. Yu, *Chemical Engineering Journal*, 2016, **283**, 956-970.
10. Y. Zhang, Y. Chen, Y. Shen, Y. Yan, J. Pan, W. Shi and L. Yu, *ChemPlusChem*, 2016, **81**, 108-118.
11. P. Viswanathan, D. W. Johnson, C. Hurley, N. R. Cameron and G. Battaglia, *Macromolecules*, 2014, **47**, 7091-7098.
12. C. R. Langford, D. W. Johnson and N. R. Cameron, *Polym. Chem.*, 2014, **5**, 6200-6206.
13. A. S. Hayward, N. Sano, S. A. Przyborski and N. R. Cameron, *Macromolecular rapid communications*, 2013, **34**, 1844-1849.
14. A. S. Hayward, A. M. Eissa, D. J. Maltman, N. Sano, S. A. Przyborski and N. R. Cameron, *Biomacromolecules*, 2013, **14**, 4271-4277.
15. S. Ungureanu, M. Birot, G. Laurent, H. Deleuze, O. Babot, B. Julián-López, M.-F. Achard, M. I. Popa, C. Sanchez and R. Backov, *Chemistry of Materials*, 2007, **19**, 5786-5796.
16. A. P. Hitchcock, C. Morin, T. Tylliszczak, I. N. Koprinarov, H. Ikeura-Sekiguchi, J. R. Lawrence and G. G. Leppard, *Surface Review and Letters*, 2002, **09**, 193-201.
17. A. Khodabandeh, R. Dario Arrua, C. T. Desire, T. Rodemann, S. A. F. Bon, S. C. Thickett and E. F. Hilder, *Polymer Chemistry*, 2016, **7**, 1803-1812.
18. R. Dario Arrua and E. F. Hilder, *RSC Adv.*, 2015, **5**, 71131-71138.
19. R. D. Arrua, A. P. Hitchcock, W. B. Hon, M. West and E. F. Hilder, *Analytical chemistry*, 2014, **86**, 2876-2881.
20. E. Candish, A. Khodabandeh, M. Gaborieau, T. Rodemann, R. A. Shellie, A. A. Gooley and E. F. Hilder, *Analytical and bioanalytical chemistry*, 2017, **409**, 2189-2199.
21. C. J. Ferguson, R. J. Hughes, D. Nguyen, B. T. T. Pham, R. G. Gilbert, A. K. Serelis, C. H. Such and B. S. Hawkett, *Macromolecules*, 2005, **38**, 2191-2204.
22. C. A. Schneider, W. S. Rasband and K. W. Eliceiri, *Nature Methods*, 2012, **9**, 671-675.
23. R. J. Carnachan, M. Bokhari, S. A. Przyborski and N. R. Cameron, *Soft Matter*, 2006, **2**, 608-616.
24. T. Ohigashi, H. Arai, T. Araki, N. Kondo, E. Shigemasa, A. Ito, N. Kosugi and M. Katoh, *Journal of Physics: Conference Series*, 2013, **463**, 012006.
25. A. P. Hitchcock, *Journal*.
26. J. Y. T. Chong, D. J. Keddie, A. Postma, X. Mulet, B. J. Boyd and C. J. Drummond, *Colloids and Surfaces A: Physicochemical and Engineering Aspects*, 2015, **470**, 60-69.
27. J. Stöhr, *NEXAFS Spectroscopy*, Springer, Berlin, 1992.
28. S. G. Urquhart, A. P. Hitchcock, A. P. Smith, H. W. Ade, W. Lidy, E. G. Rightor and G. E. Mitchell, *Journal of Electron Spectroscopy and Related Phenomena*, 1999, **100**, 119-135.
29. C. R. McNeill, B. Watts, L. Thomsen, W. J. Belcher, N. C. Greenham and P. C. Dastoor, *Nano letters*, 2006, **6**, 1202-1206.
30. A. P. Hitchcock, H. D. H. Stöver, L. M. Croll and R. F. Childs, *Australian Journal of Chemistry*, 2005, **58**, 423.